Carnitine acetyltransferase (Crat) in hunger-sensing AgRP neurons permits adaptation to calorie restriction

A Reichenbach, R Stark, M Mequinion, Sh Lockie, Mb Lemus, Rl Mynatt, S Luquet, Zb Andrews

THE FASEB JOURNAL • RESEARCH • www.fasebj.org

Carnitine acetyltransferase (Crat) in hunger-sensing AgRP neurons permits adaptation to calorie restriction

Alex Reichenbach,[*,†] Romana Stark,[*,†] Mathieu Mequinion,[*,†] Sarah H. Lockie,[*,†] Moyra B. Lemus,[*,†] Randall L. Mynatt,[‡,§] Serge Luquet,[¶] and Zane B. Andrews[*,†,1]

[*]Monash Biomedicine Discovery Institute and [†]Department of Physiology, Monash University, Clayton, Victoria, Australia; [‡]Gene Nutrient Interactions Laboratory and [§]Transgenic Core Facility, Pennington Biomedical Research Center, Louisiana State University System, Baton Rouge, Louisiana, USA; and [¶]Université of Paris Diderot, Sorbonne Paris Cité, Unité de Biologie Fonctionelle et Adaptative, Centre National de la Recherche Scientifique (CNRS) Unité Mixte de Recherche 8251, Paris, France

ABSTRACT: Hunger-sensing agouti-related peptide (AgRP) neurons ensure survival by adapting metabolism and behavior to low caloric environments. This adaption is accomplished by consolidating food intake, suppressing energy expenditure, and maximizing fat storage (nutrient partitioning) for energy preservation. The intracellular mechanisms responsible are unknown. Here we report that AgRP carnitine acetyltransferase (Crat) knockout (KO) mice exhibited increased fatty acid utilization and greater fat loss after 9 d of calorie restriction (CR). No differences were seen in mice with *ad libitum* food intake. Eleven days *ad libitum* feeding after CR resulted in greater food intake, rebound weight gain, and adiposity in AgRP Crat KO mice compared with wild-type controls, as KO mice act to restore pre-CR fat mass. Collectively, this study highlights the importance of Crat in AgRP neurons to regulate nutrient partitioning and fat mass during chronically reduced caloric intake. The increased food intake, body weight gain, and adiposity in KO mice after CR also highlights the detrimental and persistent metabolic consequence of impaired substrate utilization associated with CR. This finding may have significant implications for postdieting weight management in patients with metabolic diseases.—Reichenbach, A., Stark, R., Mequinion, M., Lockie, S. H., Lemus, M. B., Mynatt, R. L., Luquet, S., Andrews, Z. B. Carnitine acetyltransferase (Crat) in hunger-sensing AgRP neurons permits adaptation to calorie restriction. FASEB J. 32, 000–000 (2018). www.fasebj.org

KEY WORDS: rebound weight gain · body composition · RER · feeding behavior · metabolic flexibility

The neural processing of the peripheral energy state is indispensable for energy homeostasis, and disturbances in this process are linked to the emergence of metabolic disorders, including obesity and type 2 diabetes (1). Neuronal populations within the hypothalamus are all implicated in the control of energy homeostasis; however, agouti-related peptide (AgRP) neurons in the ARC are arguably the most fundamentally important population to maintain body energy homeostasis.

AgRP neurons coexpress neuropeptide Y (NPY) and GABA, and together with AgRP, all 3 play an important role in regulating food intake and energy homeostasis (2). The ablation of AgRP neurons during adulthood, which avoids development compensation, causes a dramatic loss of body weight and food intake to the point of starvation (3). Moreover, AgRP ablation during the early postnatal period permits survival but results in increased peripheral lipid utilization and lipolysis (4). In particular, AgRP/NPY neurons conserve energy by suppressing thermogenesis in white adipose tissue (5) and brown adipose tissue (BAT) (6) and reducing energy expenditure (7) *via* the CNS and the sympathetic nervous system. These studies highlight the fundamental actions of AgRP neurons to signal hunger, as well as to preferentially store lipids, particularly during energy deficits to promote survival.

AgRP itself is an endogenous antagonist at the melanocortin 4 receptor (MC4R), and central AgRP antagonism of the MC4R increases BAT temperature and glucose oxidation as indicated by the respiratory exchange ratio (RER), whereas stimulating MC receptor signaling increases lipolysis (8, 9). Moreover, NPY knockout (KO) mice have increased fat loss caused by lipolysis during calorie restriction (CR) (10). Collectively, these results show that both AgRP and NPY peptides conserve energy by regulating nutrient partitioning and utilization in peripheral tissues.

AgRP neurons are most active in response to a metabolic signature of negative energy balance that includes

ABBREVIATIONS: AgRP, agouti-related peptide; BAT, brown adipose tissue; CR, calorie restriction; Crat, carnitine acetyltransferase; FEO, food-entrainable oscillator; GFP, green fluorescent protein; KO, knockout; MC4R, melanocortin 4 receptor; NEFA, nonesterified fatty acid; NPY, neuropeptide Y; RER, respiratory exchange ratio; WT, wild type

[1] Correspondence: Monash University, Wellington Rd., Clayton, VIC 3183, Australia. E-mail: zane.andrews@monash.edu

doi: 10.1096/fj.201800634R
This article includes supplemental data. Please visit *http://www.fasebj.org* to obtain this information.

increased plasma ghrelin, free fatty acids, low glucose, low insulin, and low leptin (11–14), and they communicate with peripheral tissues through the sympathetic nervous system (5, 6, 15, 16). We recently discovered that carnitine acetyltransferase (Crat) in AgRP neurons is required to control food intake, feeding behavior, glucose clearance, lipid utilization, and AgRP protein expression during food withdrawal and refeeding. In particular, Crat in AgRP neurons regulated metabolic flexibility and facilitated a rapid switch from fatty acid to glucose oxidation upon nutrient replenishment after a single time of food withdrawal (17), indicating appropriate peripheral nutrient partitioning. These observations are consistent with studies deleting Crat in skeletal muscle, which increases fatty acid utilization and reduces metabolic flexibility, or the ability to switch metabolic substrates, during the transition from the unfed to fed state (18). This mechanism ensures that as glucose from food becomes available for oxidation, such as during refeeding, fatty acid utilization is acutely and rapidly switched off to conserve energy reserves.

Although AgRP neurons adapt to low-energy states by reducing thermogenesis and energy expenditure (4), the mechanisms responsible remain largely unknown. Research suggests that mitochondrial fission/fusion dynamics within AgRP may play a role (6), which indicates a broader role for mitochondrial metabolism within AgRP neurons as a means to detect changes in metabolic states. Indeed, our previous study showed that Crat in AgRP neurons regulates metabolic flexibility and peripheral nutrient partitioning in response to a single time of food withdrawal (17); however, the response to chronic CR remains unknown. Because CR involves multiple transitions from an unfed to fed state for a chronic period of time, we hypothesized that Crat in AgRP neurons would be critical for the adaptation to chronic energy deficit during CR. Moreover, we predict that increased fatty acid utilization in a low caloric environment would increase fat loss in AgRP Crat KO mice. To test this hypothesis, we calorie-restricted mice with an AgRP-specific deletion of Crat and analyzed changes in feeding behavior, energy expenditure, and body composition related to a low caloric environment.

MATERIALS AND METHODS

Animals

All experiments were conducted in compliance with the Monash University Animal Ethics Committee guidelines. AgRP-ires-cre mice were obtained from The Jackson Laboratory (Bar Harbor, ME, USA) AgRP$^{tm1(cre)Low/J}$ (stock no. 012899) and bred with NPY green fluorescent protein (GFP) mice (B6.FVB-Tg[Npy-hr*GFP*]1Lowl/J; stock number 006417; The Jackson Laboratory). AgRP-ires-cre::NPY GFP mice were then crossed with Crat$^{lox/lox}$ mice donated by Randall Mynatt (Pennington Biomedical Research Center, Baton Rouge, LA, USA) to delete Crat from AgRP neurons (AgRP crat KO). Before starting CR experiments, mice were kept at standard laboratory conditions with free access to food (chow diet, 8720610; Barastoc Stockfeeds, Pakenham, VIC, Australia) and water at 23°C in a 12-h light/dark cycle and were group-housed to prevent isolation stress.

Calorie restriction and *ad libitum* refeeding experiments

Male mice, 8–12 wk of age, were single-housed in specialized feeding cages (BioDaq; Research Diets, New Brunswick, NJ, USA), fitted with computer-controlled automatic gates to prevent access to feeding hoppers during CR experiments. This method also allows stress-free intervention without human interaction. After 12 d *ad libitum* feeding (inclusive acclimation period), mice were subjected to 60% CR of their average food intake during *ad libitum* conditions for 9 d. Mice gained access to food hoppers 1 h before onset of the dark phase, and individual gates closed after mice consumed 1.8 g of chow. Body weight and blood glucose levels (Accu-Chek Active; Roche Diagnostics, Tokyo, Japan) of mice were measured daily 1–2 h before refeeding. (**Fig. 1*A*** presents details of the experimental protocol.) After 9 d CR, mice were allowed access to *ad libitum* chow for 11 d to assess changes in feeding behavior.

Telemetry surgery

Mice were anesthetized with isoflurane, and anesthesia was maintained by constant nasal delivery of 2.5% isoflurane. Each animal received 50 μl Metacam (0.25 mg/ml meloxicam; Boehringer Ingelheim, Ingelheim am Rhein, Germany) before surgery to minimize postsurgery pain. Telemeter probes (Starr Life Science, Holliston, MA, USA) were implanted into the interscapular BAT, and mice were monitored for 48 h. After a 1 wk recovery period, temperature and activity were recorded every minute with Vital View 2.0 (Starr Life Science) and data averaged over 15 min.

Body composition

Body composition of mice was assessed through the EchoMRI-100H Body Composition Analyzer (EchoMRI LLC, Houston, TX, USA) by creating the average of 3 repeated scans. Body fat loss during CR was calculated as the difference of baseline (*ad libitum* fed) percent body fat and after 9 d CR. Loss and regain of body weight and lean and fat mass after 1, 4, 7, and 11 d *ad libitum* refeeding were calculated as percent change from baseline.

Metabolic phenotyping

Energy expenditure and respiratory quotient were measured with Promethion metabolic cages (Sable Systems International, North Las Vegas, NV, USA) from d 7 to 9 of CR and from d 1 to 11 during *ad libitum* refeeding. During calorie-restricted conditions, mice were subjected to the same protocol described earlier (access to 1.8 g chow commencing 1 h before onset of the dark phase).

Analysis of blood chemistry

Plasma insulin concentrations were determined through an in-house ELISA assay. Plasma concentrations of acylated and desacylated ghrelin (Mitsubishi Chemical Medience, Tokyo, Japan), glucagon (Yanaihara Institute, Fujinomiya, Japan), and corticosterone (Abnova, Heidelberg, Germany) were measured with ELISA according to manufacturer's instructions.

Nonesterified fatty acid (NEFA) concentration, ketone bodies, and triglycerides levels in plasma were measured by using a NEFA C Assay Kit (Wako Pure Chemicals, Osaka, Japan),

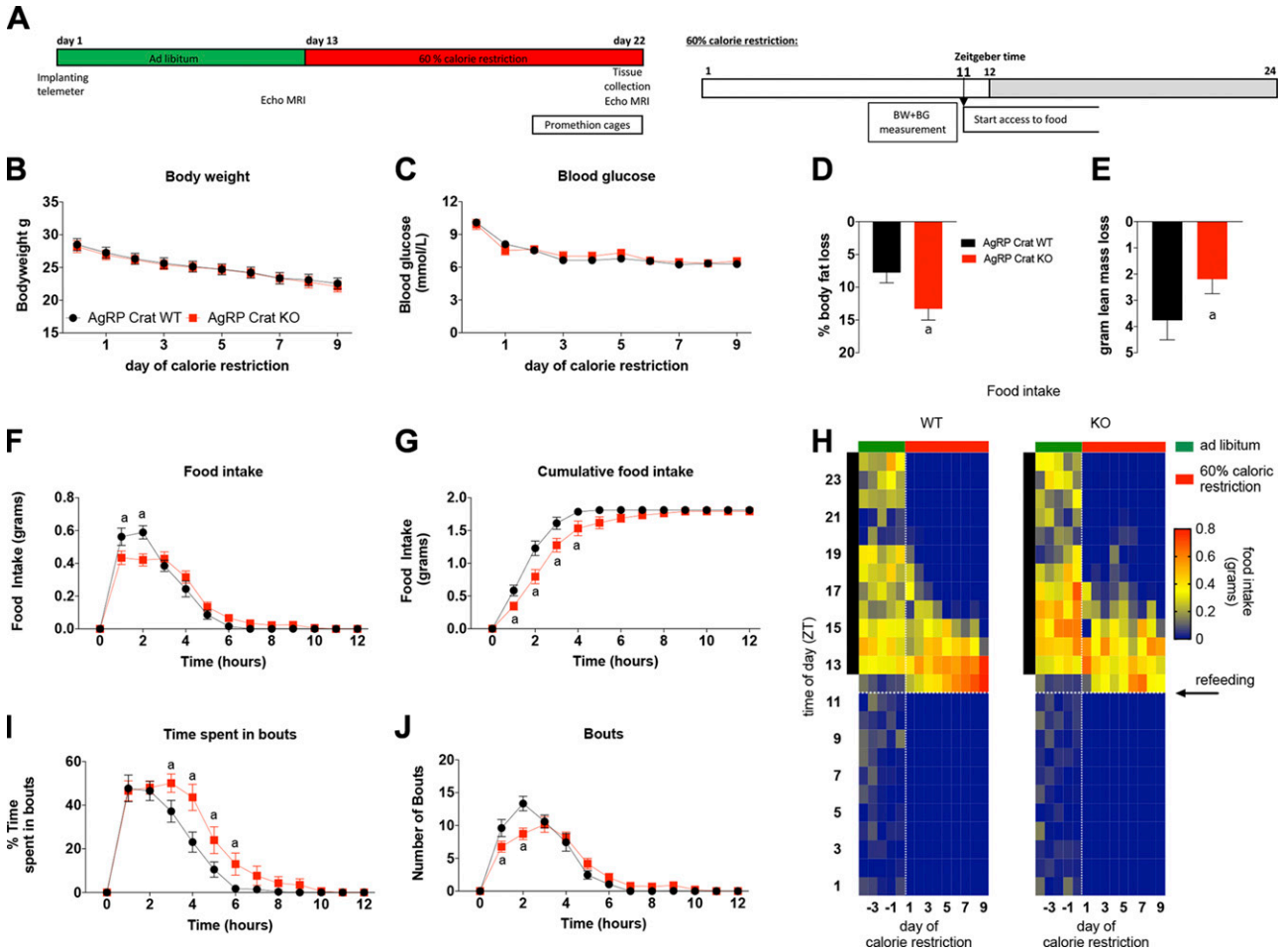

Figure 1. Crat in AgRP neurons is required for adaption of feeding behavior in response to CR. Experimental timeline of CR in BioDaq feeding cages. *A*) Three cohorts were subjected to the same feeding schedule; BAT temperature and locomotor activity were measured in cohort 1, body composition was assessed in cohort 2, and metabolic phenotype was analyzed in cohort 3. *B*, *C*) There were no differences in body weight development (*B*) or blood glucose development (*C*) between genotypes. *D–H*) Body composition examination was performed before and after the experiment, and revealed greater loss of relative fat mass (*D*) and less loss of lean mass (*E*) in KO mice during CR. Food intake (*F*), cumulative food intake during CR (*G*), and food intake under *ad libitum* fed and CR conditions shown as a heat map (*H*). Each voxel represents food intake of 1 h, each column represents a day, the black bar on the left-hand side indicates dark phase, the green bar on the top of the heat map indicates *ad libitum* access to food, and the red bar indicates restricted access to 1.8 g/24 h starting at 11 zeitgeber time (ZT), indicated by the horizontal dotted line. *I, J*) Time spent in bouts (*I*) and bouts (*J*) averaged over 9 d of CR quantify the deficits in feeding behavior. All data are expressed as means ± SEM; n = 9–11. $P < 0.05$ (ANOVA with Sidak *post hoc* analysis, 2-way repeated measures, where appropriate).

β-Hydroxybutyrate Colorimetric Assay Kit (Cayman Chemicals, Ann Arbor, MI, USA), or a Triglyceride Assay Kit (Roche/Hitachi; Roche Diagnostics), respectively.

Tissue collection

After 9 d CR or 11 d *ad libitum* refeeding, animals were deeply anesthetized with isoflurane, and blood was collected *via* cardiac puncture, and hypothalamus, gastrocnemius and soleus muscle, and liver samples were collected. Plasma collected from blood samples was stored at −80°C, and samples collected were snap frozen in liquid nitrogen.

RT-PCR

Total RNA was extracted from tissue with Qiazol (Qiazol Sciences, Germantown, MD, USA) as previously described (17). Primers were obtained from GeneWorks (Thebarton, SA, Australia): phosphoenolpyruvate carboxykinase 1 (cytosol) (5′-TGCCCAAGGCAACTTAAGGG-3′, 5′-CAGTAAACACCCCCATCGCT-3′); glucose-6-phosphatase, catalytic (5′-AGTCTTGTCAGGCATTGCTGT-3′, 5′-AAAGTCCACAGGAGGTCCAC-3′); glycogen phosphorylase, liver (5′-AAGAAGGGGTATGAGGCCAAA-3′, 5′-GACACTTGACATAGGCTTCGT-3′); glycogen synthase 2, liver (5′-AATGTGAGCCCACCAACGAT-3′, 5′-CTTCCAAAATGCACCTGGCA-3′); glycerol kinase (5′-GCAACCAGAGGGAAACCACA-3′, 5′-TAGGTCAAGCCACACCACG-3′); adipose triglyceride lipase (5′-AGAGCCCATGGTCCTCCGA-3′, 5′-AGCAAAGGGTTGGGTTGGTT-3′); diacylglycerol acyltransferase (5′-TAGAAGAGGACGAGGTGCGA-3′, 5′-GTCTTTGTCCCGGGTATGGG-3′); glycerol-3-phosphate acyltransferase, mitochondrial (5′-CCAGTGAGGACTGGGTTGAC-3′, 5′-CTCTGTGGCGTGCAGGAATA-3′); fatty acid synthase (5′-TGGGTGTGGAAGTTCGTCAG-3′, 5′-CTGTCGTGTCAGTAGCCGAG-3′); carnitine palmitoyltransferase 1a

(5′-ATCGCTTTGGGAGTCCACAT-3′, 5′-CCATCGTTAAGGCACTGGGT-3′); citrate synthase (5′-TGTAGCTCTCTCCCTTCGGT-3′, 5′-ACGAGGCAGGATGAGTTCTTG-3′); and 18S ribosomal RNA (5′-TTCCGATAACGAACGAGACTCT-3′, 5′-TGGCTGAACGCCACTTGTC-3′). Real-time quantitative PCR tests were performed by using the Real Plex4 Mastercycler (Eppendorf, Hamburg, Germany).

Liver glycogen and triglycerides

Liver glycogen and triglyceride concentrations were measured as previously described (17) with a glucose oxidase assay kit (MilliporeSigma, Burlington, MA, USA) or a triglyceride assay kit (Roche/Hitachi; Roche Diagnostics), respectively.

Statistical analysis

Statistical analyses were performed by using GraphPad Prism (La Jolla, CA, USA) for MacOS X (v.7.0b) All data are represented as means ± SEM. Two-way ANOVAs with *post hoc* tests were used to determine statistical significance between treatment and genotype. A 2-tailed, unpaired Student's *t* test was used when comparing genotype only. Linear regression analyses were performed to establish relationships between BAT temperature or locomotor activity and time. Correlation analysis was performed to determine relationships between 2 continuous variables. Values of $P < 0.05$ were considered statistically significant.

RESULTS

Crat in AgRP neurons is required for adaption of feeding behavior in response to CR

Our previous study confirmed Crat deletion in AgRP neurons and showed that Crat in AgRP neurons is required to regulate food intake, feeding microstructure, fatty acid metabolism, and energy substrate utilization after food deprivation. To determine if this scenario predisposes to metabolic impairments in models of chronic energy deficits, we exposed AgRP Crat wild-type (WT) and KO mice to a CR schedule (Fig. 1*A*). Both AgRP Crat WT and KO mice were allowed to eat 1.8 g of chow, which was assessed as ~60% of *ad libitum* food intake during a baseline period.

After mice consumed 1.8 g of chow, the computer-controlled gates closed and prevented access to the food hopper for the remainder of the 24-h period. This approach allowed CR without human intervention and additional stressors unrelated to the experimental paradigm. Interestingly, CR for 9 d did not produce a difference in body weight or blood glucose level (Fig. 1*B, C*); however, body composition analysis before and after caloric restriction in the same mice revealed that AgRP Crat KO mice lost a significantly greater percentage of body fat (Fig. 1*D*) while preserving lean mass (Fig. 1*E*). There were no differences in body weight and body composition in AgRP Crat WT or KO mice on an *ad libitum* diet during the entire experiment (Supplemental Fig. 1).

Although all mice were allowed only to eat 1.8 g of chow, AgRP Crat KO mice displayed significant differences in meal feeding microstructure, consistent with results from food withdrawal and *ad libitum* feeding behavior (17). All mice started to consume chow within a few minutes after gaining access; however, AgRP Crat KO mice took significantly longer (~8 *vs.* 4 h in WT mice) to consume most of the 1.8 g ration (Fig. 1*F–H*) and had fewer feeding bouts but spent more time in a feeding bout (Fig. 1*I, J*). Overall, WT mice adapted to the feeding regimen and changed feeding behavior accordingly by progressively consolidating their food intake into a smaller feeding window (Fig. 1*H*), whereas KO mice did not by the end of the 9 d CR.

Crat in AgRP neurons is needed to regulate nutrient partitioning and energy expenditure in response to CR

Implanting temperature probes into the interscapular BAT of mice allowed us to record real-time BAT temperature changes as well as locomotor activity in response to CR. KO mice had a slightly lower average BAT temperature during the dark phase under *ad libitum* conditions (**Fig. 2*A, B***) and failed to reduce average BAT temperature during the dark phase in response to CR (Fig. 2*A, C*). A similar effect was observed for locomotor activity in which WT mice exhibited greater locomotor activity during *ad libitum* conditions (Fig. 2*D, E*), with a 40% reduction from the first to last day of CR. KO mice showed a nonsignificant reduction in their locomotor activity by ~20% during this period (Fig. 2*D, F*), collectively suggesting greater energy conservation in WT mice during CR. To estimate energy expenditure under these advanced CR conditions, we placed mice in metabolic cages on d 7–9 of the CR protocol. The KO mice were found to have increased average energy expenditure during this period (Fig. 2*G, H*), matching the discrepancy observed in BAT temperature (Fig. 2*C*), and lower RER (Fig. 2*I, J*) compared with WT litter mates. The lower RER indicates that KO mice are preferentially utilizing fatty acids as an energy substrate, which accounts for the greater loss of fat mass during CR. This increase in fatty acid utilization during CR is consistent with results during acute food deprivation (17).

Crat in AgRP neurons affects hepatic function in response to CR

In previous food deprivation studies, we observed no differences measurable in blood glucose in WT and KO mice; however, there were significant adaptive changes in the liver of KO mice to support ongoing glucose production (17). These changes included reduced liver glycogen and elevated liver triglyceride levels, as well as changes in gene expression and the substrate contributing to gluconeogenesis. To test if similar changes occur in the calorie-restricted state, liver glycogen and triglyceride levels were measured at the end of the 9 d restriction protocol. Liver analysis revealed lower glycogen (Fig. 3*A*) but equal triglyceride (Fig. 3*B*) concentrations in AgRP Crat KO mice relative to WT mice. Liver gene expression revealed an increase in gene transcripts involved in gluconeogenesis (*Pck1*, *G6pc*) and glycogen breakdown (*Glycogen phosphorylase*), as well as carnitine

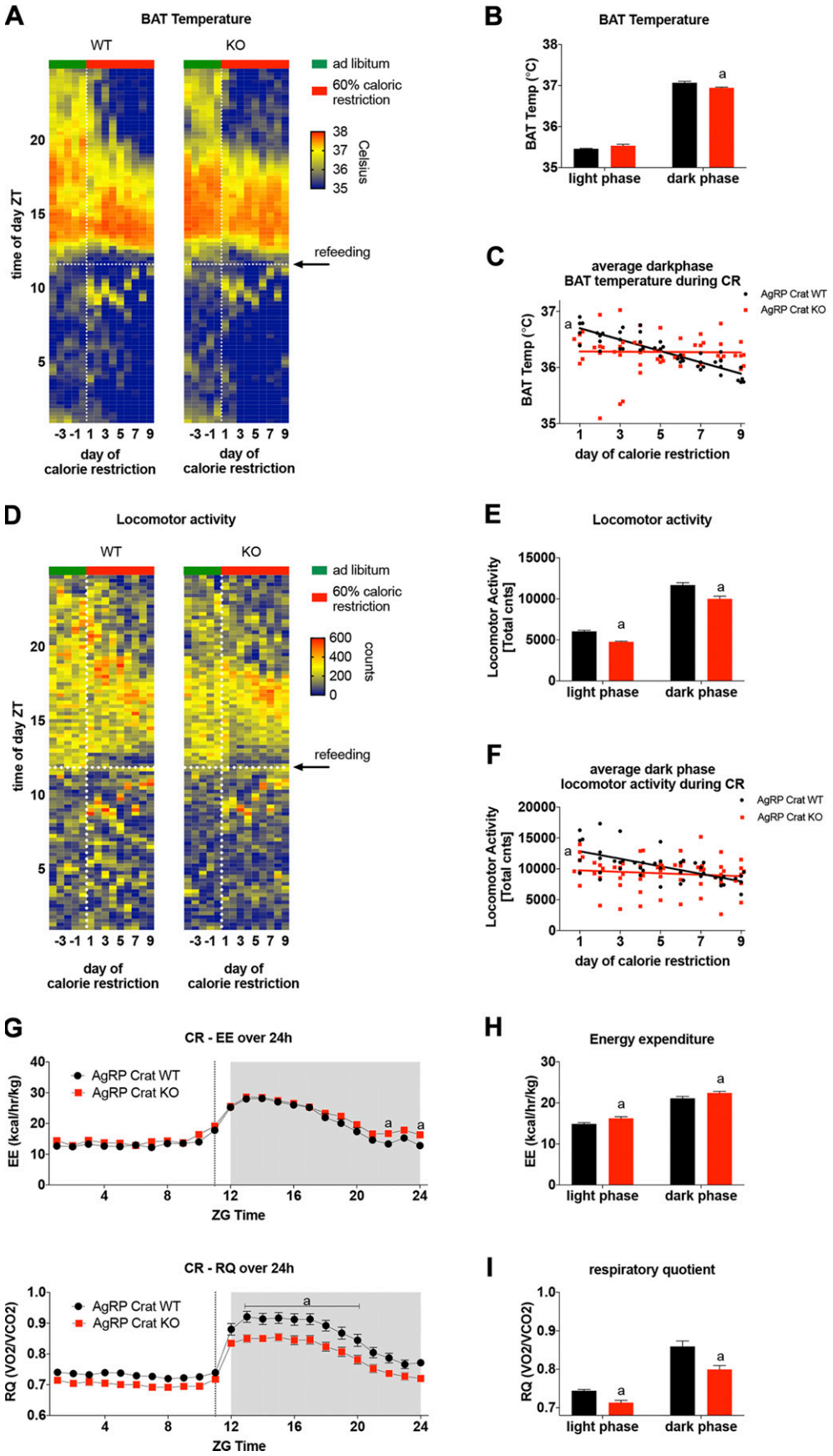

Figure 2. *A*, *D*) Crat in AgRP neurons is needed to regulate nutrient partitioning and energy expenditure in response to CR. BAT temperature (*A*) and locomotor activity (*D*) under *ad libitum* fed and CR conditions shown as a heat map. Each voxel represents average BAT temperature or cumulative locomotor activity of 15-min intervals, each column represents a day, the black bar on the left-hand side indicates the dark phase, the green bar on top of the heat map indicates *ad libitum* access to food, and the red bar indicates restricted access to 1.8 g/24 h starting at 11 zeitgeber time (ZT), indicated by the horizontal dotted line. *B*, *C*) Average BAT temperature during the light and dark phases of *ad libitum* fed animals (*B*) and regression analysis of average BAT temperature during the dark phase of 9 consecutive days CR (*C*). *E*, *F*) Total locomotor activity during the light and dark phases of *ad libitum* fed animals (*E*) and regression analysis of total dark phase locomotor activity under CR conditions (*F*). *G–J*) Average 24-h profile of energy expenditure (*G*) and respiratory quotient (RQ) (*I*) of CR d 7–9, and light and dark phase average of energy expenditure (*H*) and RQ (*J*) of this period. All data are expressed as means ± SEM; $n = 5–7$. $P < 0.05$ (ANOVA with Sidak *post hoc* analysis, 2-way repeated measures, where appropriate).

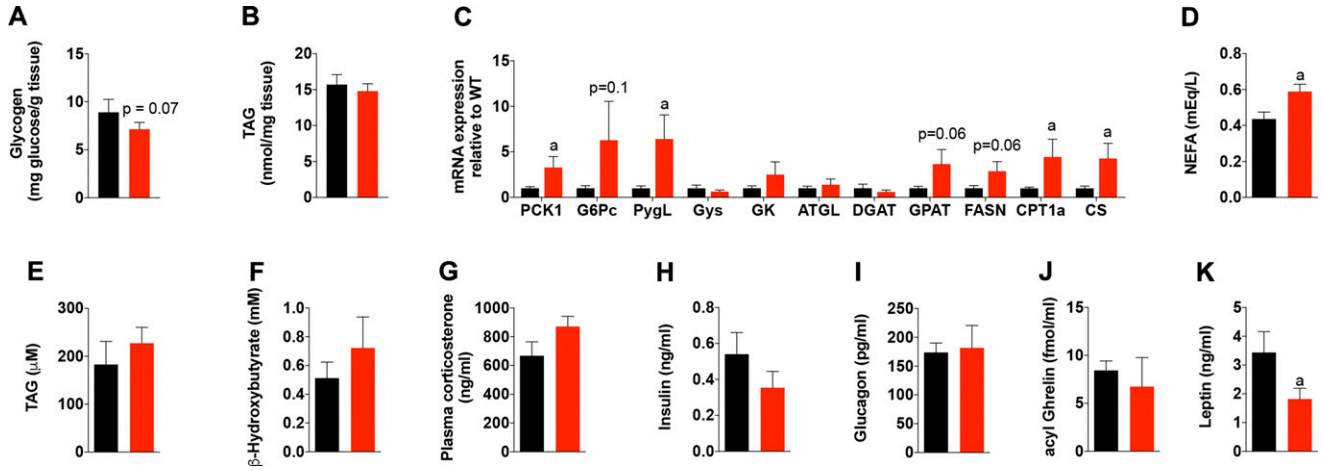

Figure 3. Crat in AgRP neurons affects hepatic function in response to CR. *A*, *B*) Liver glycogen (*A*) and triglyceride (*B*) after 9 d of CR. *C*) Hepatic gene expression of enzymes involved in gluconeogenesis, glycogenolysis, lipogenesis, and lipolysis. *H–K*) Plasma profiles after CR of metabolites: NEFA (*D*), triglycerides (*E*), and ketone bodies (*F*), and hormones: corticosterone (*G*), insulin (*H*), glucagon (*I*), acyl-ghrelin (*J*), and leptin (*K*). All data are expressed as means ± SEM; $n = 6–9$. $P < 0.05$ (2-tailed, unpaired Student's *t* test).

palmitoyltransferase 1a (*Cpt1a*) and citrate synthase (*Cs*), suggesting increased liver fatty acid oxidation and mitochondrial biogenesis in KO mice relative to WT mice (Fig. 3*C*). Interestingly, we observed an increase in *Fasn*, suggesting a possible compensatory attempt to increase *de novo* lipid synthesis due to low liver triglyceride levels after 9 d of CR, as described elsewhere (19).

Plasma NEFAs (Fig. 3*D*) were significantly higher in AgRP Crat KO mice, reflecting greater lipolytic rates; plasma triglyceride levels and ketone bodies were not significantly increased, however (Fig. 3*E, F*). No differences were observed in corticosterone, acyl ghrelin, insulin, or glucagon between AgRP Crat WT and KO mice at the end of CR (Fig. 3*G–J*). However, leptin levels were significantly lower in calorie-restricted KO mice (Fig. 3*K*), reflecting reduced adiposity.

Crat in AgRP neurons influences rebound weight gain, food intake, and adiposity after cessation of CR

At the end of CR, body weight and blood glucose levels did not differ between genotypes; however, due to changes in nutrient partitioning, KO mice had a significantly greater fat loss and less lean muscle loss. To determine if this change in body composition affected rebound weight gain, food intake, or adiposity, we observed mice for 11 d after the cessation of CR.

Compared with pre-CR body weight, WT and KO mice rapidly recovered body weight, reaching their baseline weight after 4 d refeeding, and continued to moderately gain weight (WT: 105%; KO: 109%) (**Fig. 4*A***). However, weight gain after CR significantly increased in KO mice compared with body weight at the end of CR (Fig. 4*B*). Intriguingly, after the cessation of CR, both WT mice and KO mice dramatically increased their 24 h food intake to ~165 and 150% of baseline *ad libitum* food intake, respectively. With time, WT mice reduced their daily food intake to below baseline levels after 7 d *ad libitum* refeeding; however, KO mice continued to consume more compared with *ad libitum* food intake, resulting in significantly greater chow consumption at the end of the experimental period (Fig. 4*C, D*).

Body composition analysis with ECHO MRI dissociated weight gain in lean mass from that in fat mass (Fig. 4*E*). This analysis showed that the increase in body weight the first day after cessation of CR is due to complete restoration of pre-CR lean mass. Although WT mice had slightly reduced lean mass thereafter, KO mice maintained the increased lean mass to the end of the experiment (Fig. 4*F*). The restoration of fat mass after CR takes longer, with WT mice reaching pre-CR adiposity between 4 and 7 d *ad libitum* refeeding. Despite gaining more absolute fat mass (Fig. 4*H*), KO mice did not reach their pre-CR adiposity level until after 11 d *ad libitum* refeeding (Fig. 4*G*), due to the greater fat loss during CR (Fig. 4*G*, compared with Fig. 1*D*). Dulloo *et al.* (20) suggest that the interplay between mechanisms regulating fat and protein mass, including the ratio of secreted adipokines and myokines, may regulate body composition and determine food intake to regain fat and lean mass. In our studies, KO mice gained more relative fat and lean mass compared with WT controls and also consumed more food. Furthermore, the significant inverse correlation between the relative change in fat mass and change in food intake (Fig. 4*I, J*) suggests that elevated food intake in KO mice in the post-CR period is to restore adiposity levels to pre-CR levels and not body weight per se (Fig. 4*K, L*). This concept is in line with leptin from adipose tissue as an endocrine signal that communicates long-term energy availability to the brain (21, 22).

We therefore analyzed circulating leptin from plasma of refed mice (**Fig. 5*A***) and found no difference between genotypes for leptin levels or for the correlation between circulating leptin levels and fat mass (Fig. 5*D, E*). Measuring insulin (Fig. 5*B*) and NEFA (Fig. 5*C*) from the same animals also revealed no differences between genotypes. Metabolic analysis during *ad libitum* refeeding found that

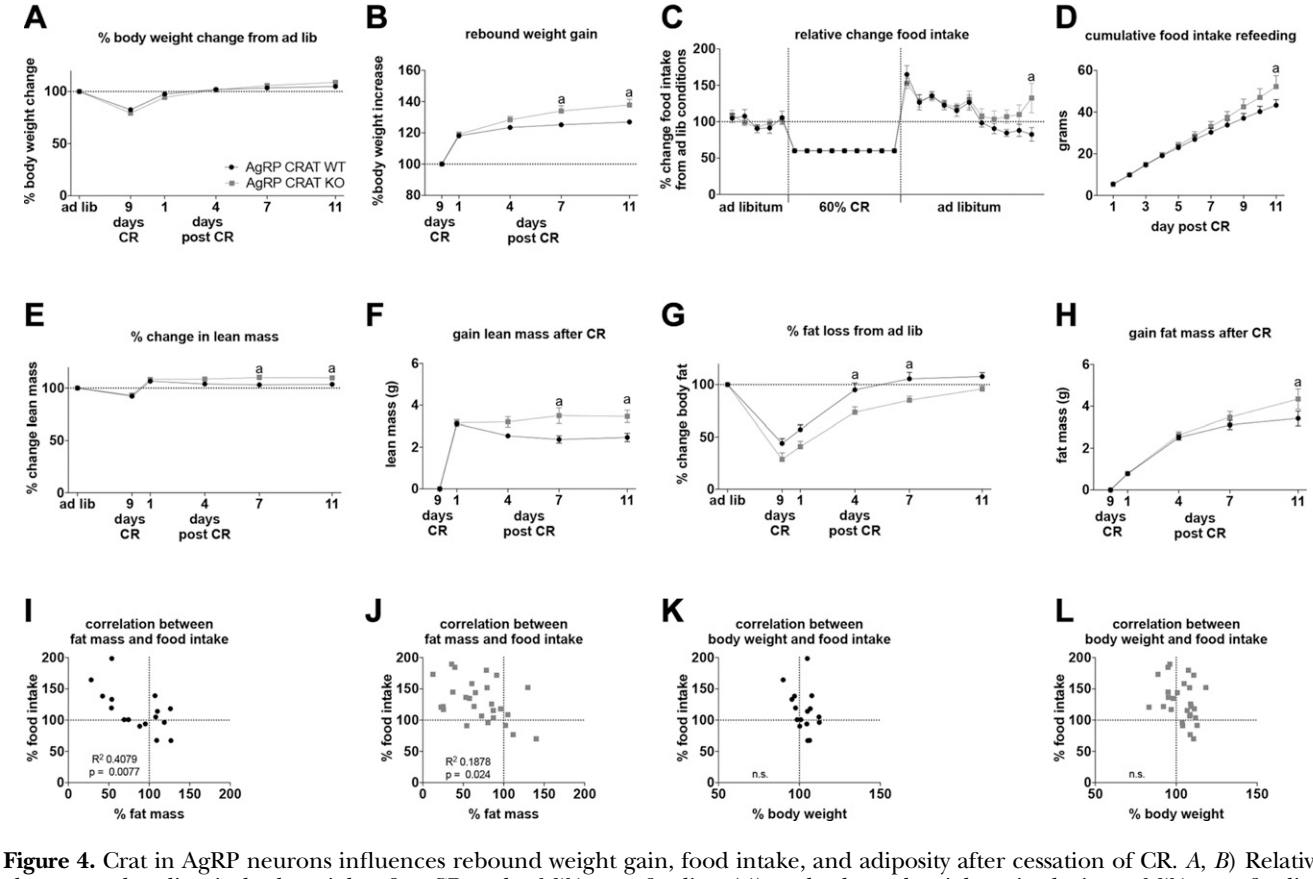

Figure 4. Crat in AgRP neurons influences rebound weight gain, food intake, and adiposity after cessation of CR. *A*, *B*) Relative changes to baseline in body weight after CR and *ad libitum* refeeding (*A*) and rebound weight gain during *ad libitum* refeeding (*B*). *C*, *D*) Changes in average 24-h food intake relative to baseline *ad libitum* fed conditions (*C*) and cumulative food intake during *ad libitum* refeeding (*D*). *E–H*) Changes relative to baseline in lean mass (*E*) and fat mass (*G*) after CR and ad libitum refeeding and gain in lean mass (*F*) and fat mass (*H*) during *ad libitum* refeeding. *I–L*) Correlation between changes in food intake and changes in fat mass (*I*, *J*) and correlation between changes in food intake and changes in body weight (*K*, *L*). All data are expressed as means ± SEM; $n = 9–11$. $P < 0.05$ (ANOVA with Sidak *post hoc* analysis, 2-way repeated measures, where appropriate).

there are no genotype differences in energy expenditure (Fig. 5*G*). Furthermore, KO mice have lower RER compared with WT controls (Fig. 5*F*, *H*), showing a persistent increase in fatty acid utilization 11 d post-CR. Despite this persistent increase in lipid utilization, KO mice consume more food and gain fat mass compared with WT mice to restore pre-CR adiposity levels.

DISCUSSION

The metabolic flexibility to acutely switch fatty acid to glucose utilization during refeeding represents an important mechanism referred to as "nutrient partitioning" that helps store energy-rich fatty acids and maximizes energy conservation until required. Our previous studies showed that Crat in AgRP neurons is important to regulate metabolic flexibility and peripheral nutrient partitioning (17). Here we show that Crat-mediated metabolic signaling in AgRP neurons regulates metabolic adaptation to a chronic state of low caloric intake (60% CR) by regulating meal feeding structure, BAT thermogenesis, peripheral energy expenditure, and energy substrate utilization.

Although Crat deletion from AgRP neurons does not affect body weight loss or blood glucose level during CR, it causes a greater loss of body fat. Intriguingly, rebound weight gain, lean and fat mass, and food intake all increased, and fatty acid utilization remained high after the cessation of CR in KO mice compared with WT controls. These studies suggest that Crat in AgRP neurons regulates peripheral nutrient partitioning to preserve lipid stores and suppress energy expenditure during the chronic nutrient shortfall associated with CR. It is important to note that we observed no differences in body weight, lean mass, or fat mass in AgRP Crat WT and KO mice on a normal *ad libitum* diet, indicating that the observed phenotype is not simply due to the deletion of Crat from AgRP neurons. The phenotype in KO mice only manifests once the mice are subjected to CR, at a time when AgRP neurons become more active to restore energy homeostasis.

These studies also highlight that chronic impairment in nutrient partitioning during CR can affect rebound weight gain, rebound food intake, and rebound adiposity. Such an observation may have implications for rebound weight gain after diet-restricted weight loss interventions in humans. This finding is especially important considering metabolic diseases such as diabetes, nonalcoholic fatty liver disease, and dyslipidemia can develop due to inappropriate nutrient "fate" without significant changes in body weight (23–26).

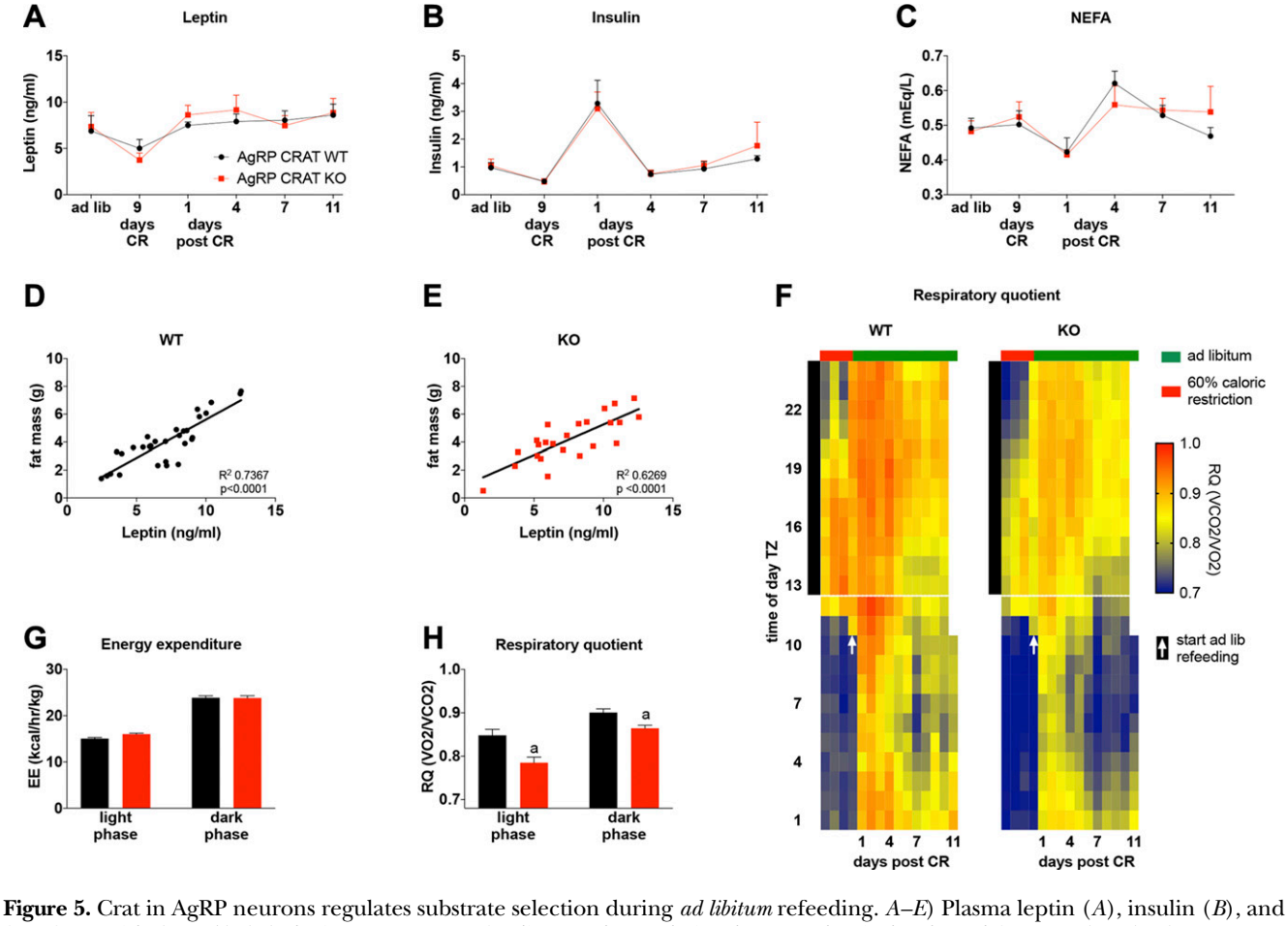

Figure 5. Crat in AgRP neurons regulates substrate selection during *ad libitum* refeeding. *A–E*) Plasma leptin (*A*), insulin (*B*), and free fatty acids (NEFA) (*C*) during *ad libitum* refeeding, and correlation between leptin levels and fat mass (*D, E*). *F*) Heat map depicting temporal changes in respiratory quotient (RQ) during transition from calorie restricted to *ad libitum* refed conditions. Each voxel represents average RQ of 1 h, each column represents a day, the black bar on the left-hand side indicates the dark phase, the red bar on the top indicates restricted access to 1.8 g/24 h starting at 11 zeitgeber time (ZT), indicated by the horizontal white line, *ad libitum* access to food is indicated by the green bar on top of the heat map, and start of *ad libitum* refeeding is indicated by the white arrows. *G, H*) Average energy expenditure (*G*) and RQ (*H*) of the light and dark phases during *ad libitum* refeeding. All data are expressed as means ± SEM; $n = 9–11$. $P < 0.05$ (ANOVA with Sidak *post hoc* analysis, 2-way repeated measures, where appropriate).

In terms of meal feeding structure, WT mice adapted over the course of the CR protocol to quickly consume food, which was always introduced at the same time of the day during CR, an effect that is supported by previous studies (27). The finding that AgRP Crat KO mice did not show the same temporal adaptation over the course of CR implies that Crat in AgRP neurons is crucial for assessment of food availability and may be involved in a food-entrainable oscillator (FEO) (28). Tan *et al.* (29) showed that ablating AgRP neurons delays food intake under a daytime restricted feeding regimen, as well as abolishes the food-anticipatory activity, an important feature of the FEO. In support of this theory, KO mice did not exhibit a similar temporal adaptation in BAT temperature, locomotor activity, or energy expenditure, all of which are important functions controlled by AgRP neurons (6, 7, 9). Given that Crat in AgRP neurons is required for metabolic flexibility and peripheral nutrient partitioning, it is tempting to speculate that the metabolic processing of incoming nutrients *via* Crat is a key component of the FEO. There is evidence to support this claim because feeding time influences metabolism (30–32) and circadian cycles influence mitochondrial rate-limiting enzymes and nutrient utilization (33). In a proteomic screen of AgRP neurons from WT and KO mice, we observed numerous differences in mitochondrial enzymes, NAD+-regulating enzymes, and differences in protein acetylation (17), all of which affect NAD+ bioavailability and modulate mitochondrial oxidative function across cycles of food deprivation and feeding (34). Collectively, these results suggest that Crat in AgRP neurons may be vital for the accurate assessment of peripheral nutrient availability and subsequent nutrient partitioning, which enables behavioral and metabolic adaptation to chronic low caloric environments to ensure and maximize energy conservation.

In previous experiments, we showed that AgRP Crat KO mice exhibit a shift toward increased fatty acid utilization and an attenuated switch to glucose oxidation with nutrient replenishment after food withdrawal (17). Our observations herein show that prolonged preferential fatty acid utilization and increased lipolysis, as indicated by lower RER and increased NEFAs, respectively, during

chronic low caloric conditions result in increased body fat loss. This shift toward fatty acid utilization might be facilitated by reduced AgRP-mediated antagonism of MC4R, resulting in augmented MC4R signaling and increased lipolysis (8, 9). Nevertheless, our results are consistent with the ablation of AgRP or NPY neurons on substrate utilization and nutrient partitioning (4, 10).

Consistent with our previous report (17), we observed a hepatic mRNA profile with increased gluconeogenic and glycogenolytic genes, as well as genes suggesting increased liver fatty acid oxidation and mitochondrial biogenesis in KO mice to support gluconeogenesis (35). The differences in hepatic gene profile are supported by a lower glycogen concentration in KO mice. Furthermore, we observed an increase in *Fasn* that suggests an increase in *de novo* lipid synthesis. Indeed, it has been reported that *de novo* lipid synthesis is elevated to meet the lipid demand during CR (19).

Although the integrated neural circuit responsible for the effect of CR on lipolysis and fat utilization remains unknown, it presumably involves impaired sympathetic nervous system–mediated communication with peripheral tissues as seen in previous studies on AgRP function (6, 16, 17, 36). Furthermore, an AgRP->PVN pathway subpopulation is required to drive positive reinforcement after food intake in caloric-depleted mice (37, 38). Moreover, food ingestion also alleviates a negative valence signal conferred by persistent AgRP neuronal activity (39). Thus, these combined actions in WT mice presumably underlie the temporal adaptation to consume food quickly over the 9-d restriction protocol. The finding that KO mice take longer to consume the same amount suggests altered processing in response to these valence cues, which may affect motivational aspects of food intake during a state of homeostatic need. Indeed, fewer feeding bouts 4 h after food access and reduced food consumption despite more time in a given feeding bout suggests that deletion of Crat in AgRP neurons affects the motivation for food intake. Future studies are required to address this suggestion.

We propose that Crat may be a critical enzyme that enables AgRP neurons to act as energy calculators, as proposed by Beutler *et al.* (40), integrating information on acute changes in energy balance and regulating substrate utilization in response. Indeed, we have previously shown that deleting Crat in AgRP neurons impairs the switch in substrate utilization upon refeeding but does not disturb energy homeostasis under *ad libitum* fed conditions (17). Furthermore, we found no differences in the orexigenic hormone ghrelin and lower levels of leptin in calorie-restricted animals, supporting the notion that AgRP neurons regulate energy homeostasis through multiple mechanisms on different time scales. In our view, Crat activity in AgRP neurons links food availability with peripheral energy metabolism (4, 17), ensuring appropriate adaptative nutrient partititoning during CR. In that view perception of food quality and availability and later on calorie intake would have a dynamic action onto AgRP neuron activity through Crat activity allowing for adaptive nutrient partitioning.

Our post-CR *ad libitum* refeeding experiments found that AgRP Crat KO mice, despite losing more fat under CR conditions, are capable of regenerating fat mass by increasing food intake until prediet adiposity is reached, similar to WT controls. Surprisingly, despite the greater loss of body fat at the end of CR, KO mice had no difference in body weight due to a preservation of lean mass and even an increase in their relative lean mass during post-CR *ad libitum* feeding, leading to greater rebound body weight compared with WT mice. In support of this outcome, AgRP activation is associated with increased circulating plasma myostatin (41), which is a negative regulator of muscle mass. Because the inhibition of myostatin increases muscle mass in mice (42), any influence on the ability of AgRP neurons to regulate myostatin may affect the preservation or restoration of lean mass; we suggest that the deletion of Crat in AgRP neurons represents one such influence over AgRP neurons. This finding might have implications for muscle degenerative diseases such as cachexia or muscle dystrophy, but further research is needed, as CR has differential effects on muscles dependent on strain, sex, and time (43). Recent studies also suggest osteocytes act as a body weight sensor, regulating food intake independent of leptin to maintain body weight (44). The relative increase in lean mass elevates basal metabolic rate (45, 46), which is known to influence food intake (47), offering an explanation for increased food intake in AgRP Crat KO mice during *ad libitum* refeeding.

In summary, Crat deletion in AgRP neurons promoted a shift toward increased fatty acid utilization, which persisted during the post-CR feeding period. This chronic impairment in nutrient partitioning affected food intake, body composition, adiposity, and rebound weight gain after a period of CR, which has significant implications for people in weight loss programs, especially considering metabolic inflexibility in obesity (26). Collectively, our results show that Crat in AgRP neurons is crucial for adaptation to low caloric environments. In particular, this goal is achieved by adjusting feeding behavior to consume food quickly, control nutrient partitioning and substrate selection to preserve fat stores, and regulate energy expenditure to conserve energy. Finally, beyond dieting, chronic CR has been repeatedly shown to enhance life span in several species (48–51). It is tempting to speculate that crat-metabolism in AgRP neurons is an important mechanism through which CR facilitates a global shift in peripheral substrate utilization and a whole-body optimization of fuel partitioning allowing for reduction of oxidative damage. This outcome highlights the fact that Crat in AgRP neurons acts as an integrator of acute changes to adapt metabolism and behavior by regulating nutrient partitioning, and that defects of this mechanism affect body weight and adiposity with implications for metabolic diseases. FJ

ACKNOWLEDGMENTS

The authors thank Doug Compton (Research Diets, New Brunswick, NJ, USA) for helping construct and establish the BioDaq feeding cages. This study was supported by an Australian National Health and Medical Research Council (NHMRC) grant and fellowship (1126724, 1084344) to Z.B.A. This work used the Pennington Biomedical Research Center

Transgenic Core, which is supported, in part, by the U.S. National Institutes of Health (NIH) Centers of Biomedical Research Excellence (8P20GM103528) and the NIH Nutrition Obesity Research Centers (2P30-DK072476-11A1). A.R. is supported through an Australian Government Research Training Program Scholarship. S.H.L. and R.S. are supported by an Australian NHMRC Early Career Research Fellowship. The authors declare no conflicts of interest.

AUTHOR CONTRIBUTIONS

A. Reichenbach and Z. B. Andrews conceived the idea, designed and performed the experiments, analyzed data, and wrote the manuscript; Z. B. Andrews supervised and coordinated the project; S. Luquet helped design experiments; R. Stark, M. Mequinion, S. H. Lockie, and M. B. Lemus contributed to perform experiments; R. L. Mynatt provided the Crat floxed mouse model; A. Reichenbach, S. Luquet, and Z. B. Andrews discussed results and edited the manuscript; and all authors read and approved the manuscript.

REFERENCES

1. O'Rahilly, S., and Farooqi, I. S. (2008) Human obesity: a heritable neurobehavioral disorder that is highly sensitive to environmental conditions. *Diabetes* **57**, 2905–2910
2. Krashes, M. J., Shah, B. P., Koda, S., and Lowell, B. B. (2013) Rapid versus delayed stimulation of feeding by the endogenously released AgRP neuron mediators GABA, NPY, and AgRP. *Cell Metab.* **18**, 588–595
3. Luquet, S., Perez, F. A., Hnasko, T. S., and Palmiter, R. D. (2005) NPY/AgRP neurons are essential for feeding in adult mice but can be ablated in neonates. *Science* **310**, 683–685
4. Joly-Amado, A., Denis, R. G., Castel, J., Lacombe, A., Cansell, C., Rouch, C., Kassis, N., Dairou, J., Cani, P. D., Ventura-Clapier, R., Prola, A., Flamment, M., Foufelle, F., Magnan, C., and Luquet, S. (2012) Hypothalamic AgRP-neurons control peripheral substrate utilization and nutrient partitioning. *EMBO J.* **31**, 4276–4288
5. Dodd, G. T., Andrews, Z. B., Simonds, S. E., Michael, N. J., DeVeer, M., Bruning, J. C., Spanswick, D., Cowley, M. A., and Tiganis, T. (2017) A hypothalamic phosphatase switch coordinates energy expenditure with feeding. *Cell Metab.* **26**, 375–393.e7; erratum: 577
6. Ruan, H. B., Dietrich, M. O., Liu, Z. W., Zimmer, M. R., Li, M. D., Singh, J. P., Zhang, K., Yin, R., Wu, J., Horvath, T. L., and Yang, X. (2014) O-GlcNAc transferase enables AgRP neurons to suppress browning of white fat. *Cell* **159**, 306–317
7. Shi, Y. C., Lau, J., Lin, Z., Zhang, H., Zhai, L., Sperk, G., Heilbronn, R., Mietzsch, M., Weger, S., Huang, X. F., Enriquez, R. F., Baldock, P. A., Zhang, L., Sainsbury, A., Herzog, H., and Lin, S. (2013) Arcuate NPY controls sympathetic output and BAT function via a relay of tyrosine hydroxylase neurons in the PVN. *Cell Metab.* **17**, 236–248
8. Nogueiras, R., Wiedmer, P., Perez-Tilve, D., Veyrat-Durebex, C., Keogh, J. M., Sutton, G. M., Pfluger, P. T., Castaneda, T. R., Neschen, S., Hofmann, S. M., Howles, P. N., Morgan, D. A., Benoit, S. C., Szanto, I., Schrott, B., Schürmann, A., Joost, H. G., Hammond, C., Hui, D. Y., Woods, S. C., Rahmouni, K., Butler, A. A., Farooqi, I. S., O'Rahilly, S., Rohner-Jeanrenaud, F., and Tschöp, M. H. (2007) The central melanocortin system directly controls peripheral lipid metabolism. *J. Clin. Invest.* **117**, 3475–3488
9. Brito, M. N., Brito, N. A., Baro, D. J., Song, C. K., and Bartness, T. J. (2007) Differential activation of the sympathetic innervation of adipose tissues by melanocortin receptor stimulation. *Endocrinology* **148**, 5339–5347
10. Park, S., Komatsu, T., Kim, S. E., Tanaka, K., Hayashi, H., Mori, R., and Shimokawa, I. (2017) Neuropeptide Y resists excess loss of fat by lipolysis in calorie-restricted mice: a trait potential for the life-extending effect of calorie restriction. *Aging Cell* **16**, 339–348
11. Lockie, S. H., and Andrews, Z. B. (2013) The hormonal signature of energy deficit: increasing the value of food reward. *Mol. Metab.* **2**, 329–336
12. Mandelblat-Cerf, Y., Ramesh, R. N., Burgess, C. R., Patella, P., Yang, Z., Lowell, B. B., and Andermann, M. L. (2015) Arcuate hypothalamic AgRP and putative POMC neurons show opposite changes in spiking across multiple timescales. *eLife* **4**
13. Joly-Amado, A., Cansell, C., Denis, R. G., Delbes, A. S., Castel, J., Martinez, S., and Luquet, S. (2014) The hypothalamic arcuate nucleus and the control of peripheral substrates. *Best Pract. Res. Clin. Endocrinol. Metab.* **28**, 725–737
14. Andermann, M. L., and Lowell, B. B. (2017) Toward a wiring diagram understanding of appetite control. *Neuron* **95**, 757–778
15. Nogueiras, R., Lopez, M., and Dieguez, C. (2009) Regulation of lipid metabolism by energy availability: a role for the central nervous system. *Obes. Rev.* **11**, 185–201
16. Shi, Z., Madden, C. J., and Brooks, V. L. (2017) Arcuate neuropeptide Y inhibits sympathetic nerve activity via multiple neuropathways. *J. Clin. Invest.* **127**, 2868–2880
17. Reichenbach, A., Stark, R., Mequinion, M., Denis, R. R. G., Goularte, J. F., Clarke, R. E., Lockie, S. H., Lemus, M. B., Kowalski, G. M., Bruce, C. R., Huang, C., Schittenhelm, R. B., Mynatt, R. L., Oldfield, B. J., Watt, M. J., Luquet, S., and Andrews, Z. B. (2018) AgRP neurons require carnitine acetyltransferase to regulate metabolic flexibility and peripheral nutrient partitioning. *Cell Rep.* **22**, 1745–1759
18. Muoio, D. M., Noland, R. C., Kovalik, J. P., Seiler, S. E., Davies, M. N., DeBalsi, K. L., Ilkayeva, O. R., Stevens, R. D., Kheterpal, I., Zhang, J., Covington, J. D., Bajpeyi, S., Ravussin, E., Kraus, W., Koves, T. R., and Mynatt, R. L. (2012) Muscle-specific deletion of carnitine acetyltransferase compromises glucose tolerance and metabolic flexibility. *Cell Metab.* **15**, 764–777
19. Bruss, M. D., Khambatta, C. F., Ruby, M. A., Aggarwal, I., and Hellerstein, M. K. (2010) Calorie restriction increases fatty acid synthesis and whole body fat oxidation rates. *Am. J. Physiol. Endocrinol. Metab.* **298**, E108–E116
20. Dulloo, A. G., Jacquet, J., Montani, J. P., and Schutz, Y. (2015) How dieting makes the lean fatter: from a perspective of body composition autoregulation through adipostats and proteinstats awaiting discovery. *Obes. Rev.* **16**(Suppl. 1), 25–35
21. Stern, J. H., Rutkowski, J. M., and Scherer, P. E. (2016) Adiponectin, leptin, and fatty acids in the maintenance of metabolic homeostasis through adipose tissue crosstalk. *Cell Metab.* **23**, 770–784
22. Rosen, E. D., and Spiegelman, B. M. (2014) What we talk about when we talk about fat. *Cell* **156**, 20–44
23. Darabian, S., Backlund, J. Y., Cleary, P. A., Sheidaee, N., Bebu, I., Lachin, J. M., and Budoff, M. J.; DCCT/EDIC Research Group. (2016) Significance of epicardial and intrathoracic adipose tissue volume among type 1 diabetes patients in the DCCT/EDIC: a pilot study. *PLoS One* **11**, e0159958
24. Padwal, R., Leslie, W. D., Lix, L. M., and Majumdar, S. R. (2016) Relationship among body fat percentage, body mass index, and all-cause mortality: a cohort study. *Ann. Intern. Med.* **164**, 532–541
25. Gastaldelli, A. (2017) Insulin resistance and reduced metabolic flexibility: cause or consequence of NAFLD? *Clin. Sci. (Lond.)* **131**, 2701–2704
26. Goodpaster, B. H., and Sparks, L. M. (2017) Metabolic flexibility in health and disease. *Cell Metab.* **25**, 1027–1036
27. Acosta-Rodriguez, V. A., de Groot, M. H. M., Rijo-Ferreira, F., Green, C. B., and Takahashi, J. S. (2017) Mice under caloric restriction self-impose a temporal restriction of food intake as revealed by an automated feeder system. *Cell Metab.* **26**, 267–277.e2
28. Carneiro, B. T., and Araujo, J. F. (2009) The food-entrainable oscillator: a network of interconnected brain structures entrained by humoral signals? *Chronobiol. Int.* **26**, 1273–1289
29. Tan, K., Knight, Z. A., and Friedman, J. M. (2014) Ablation of AgRP neurons impairs adaption to restricted feeding. *Mol. Metab.* **3**, 694–704
30. Shamsi, N. A., Salkeld, M. D., Rattanatray, L., Voultsios, A., Varcoe, T. J., Boden, M. J., and Kennaway, D. J. (2014) Metabolic consequences of timed feeding in mice. *Physiol. Behav.* **128**, 188–201
31. Zwighaft, Z., Aviram, R., Shalev, M., Rousso-Noori, L., Kraut-Cohen, J., Golik, M., Brandis, A., Reinke, H., Aharoni, A., Kahana, C., and Asher, G. (2015) Circadian clock control by polyamine levels through a mechanism that declines with age. *Cell Metab.* **22**, 874–885
32. Mauvoisin, D., Atger, F., Dayon, L., Núñez Galindo, A., Wang, J., Martin, E., Da Silva, L., Montoliu, I., Collino, S., Martin, F. P., Ratajczak, J., Cantó, C., Kussmann, M., Naef, F., and Gachon, F. (2017) Circadian and feeding rhythms orchestrate the diurnal liver acetylome. *Cell Reports* **20**, 1729–1743
33. Neufeld-Cohen, A., Robles, M. S., Aviram, R., Manella, G., Adamovich, Y., Ladeuix, B., Nir, D., Rousso-Noori, L., Kuperman, Y., Golik, M.,

Mann, M., and Asher, G. (2016) Circadian control of oscillations in mitochondrial rate-limiting enzymes and nutrient utilization by PERIOD proteins. *Proc. Natl. Acad. Sci. USA* **113**, E1673–E1682
34. Peek, C. B., Affinati, A. H., Ramsey, K. M., Kuo, H. Y., Yu, W., Sena, L. A., Ilkayeva, O., Marcheva, B., Kobayashi, Y., Omura, C., Levine, D. C., Bacsik, D. J., Gius, D., Newgard, C. B., Goetzman, E., Chandel, N. S., Denu, J. M., Mrksich, M., and Bass, J. (2013) Circadian clock NAD+ cycle drives mitochondrial oxidative metabolism in mice. *Science* **342**, 1243417
35. Jackowski, S., and Leonardi, R. (2014) Deregulated coenzyme A, loss of metabolic flexibility and diabetes. *Biochem. Soc. Trans.* **42**, 1118–1122
36. Kuperman, Y., Weiss, M., Dine, J., Staikin, K., Golani, O., Ramot, A., Nahum, T., Kühne, C., Shemesh, Y., Wurst, W., Harmelin, A., Deussing, J. M., Eder, M., and Chen, A. (2016) CRFR1 in AgRP neurons modulates sympathetic nervous system activity to adapt to cold stress and fasting. *Cell Metab.* **23**, 1185–1199
37. Garfield, A. S., Li, C., Madara, J. C., Shah, B. P., Webber, E., Steger, J. S., Campbell, J. N., Gavrilova, O., Lee, C. E., Olson, D. P., Elmquist, J. K., Tannous, B. A., Krashes, M. J., and Lowell, B. B. (2015) A neural basis for melanocortin-4 receptor-regulated appetite. *Nat. Neurosci.* **18**, 863–871
38. Chen, Y., Lin, Y. C., Zimmerman, C. A., Essner, R. A., and Knight, Z. A. (2016) Hunger neurons drive feeding through a sustained, positive reinforcement signal. *eLife* **5**
39. Betley, J. N., Xu, S., Cao, Z. F. H., Gong, R., Magnus, C. J., Yu, Y., and Sternson, S. M. (2015) Neurons for hunger and thirst transmit a negative-valence teaching signal. *Nature* **521**, 180–185
40. Beutler, L. R., Chen, Y., Ahn, J. S., Lin, Y. C., Essner, R. A., and Knight, Z. A. (2017) Dynamics of gut-brain communication underlying hunger. *Neuron.* **96**, 461–475.e5
41. Steculorum, S. M., Ruud, J., Karakasilioti, I., Backes, H., Engström Ruud, L., Timper, K., Hess, M. E., Tsaousidou, E., Mauer, J., Vogt, M. C., Paeger, L., Bremser, S., Klein, A. C., Morgan, D. A., Frommolt, P., Brinkkötter, P. T., Hammerschmidt, P., Benzing, T., Rahmouni, K., Wunderlich, F. T., Kloppenburg, P., and Brüning, J. C. (2016) AgRP neurons control systemic insulin sensitivity via myostatin expression in brown adipose tissue. *Cell* **165**, 125–138
42. Whittemore, L. A., Song, K., Li, X., Aghajanian, J., Davies, M., Girgenrath, S., Hill, J. J., Jalenak, M., Kelley, P., Knight, A., Maylor, R., O'Hara, D., Pearson, A., Quazi, A., Ryerson, S., Tan, X. Y., Tomkinson, K. N., Veldman, G. M., Widom, A., Wright, J. F., Wudyka, S., Zhao, L., and Wolfman, N. M. (2003) Inhibition of myostatin in adult mice increases skeletal muscle mass and strength. *Biochem. Biophys. Res. Commun.* **300**, 965–971
43. Boldrin, L., Ross, J. A., Whitmore, C., Doreste, B., Beaver, C., Eddaoudi, A., Pearce, D. J., and Morgan, J. E. (2017) The effect of calorie restriction on mouse skeletal muscle is sex, strain and time-dependent. *Sci. Rep.* **7**, 5160
44. Jansson, J. O., Palsdottir, V., Hagg, D. A., Schele, E., Dickson, S. L., Anesten, F., Bake, T., Montelius, M., Bellman, J., Johansson, M. E., Cone, R. D., Drucker, D. J., Wu, J., Aleksic, B., Tornqvist, A. E., Sjogren, K., Gustafsson, J. A., Windahl, S. H., and Ohlsson, C. (2017) Body weight homeostat that regulates fat mass independently of leptin in rats and mice. *Proc. Natl. Acad. Sci. USA* **115**, 427–432
45. Hopkins, M., Finlayson, G., Duarte, C., Whybrow, S., Ritz, P., Horgan, G. W., Blundell, J. E., and Stubbs, R. J. (2016) Modelling the associations between fat-free mass, resting metabolic rate and energy intake in the context of total energy balance. *Int. J. Obes.* **40**, 312–318
46. Weise, C. M., Thiyyagura, P., Reiman, E. M., Chen, K., and Krakoff, J. (2015) A potential role for the midbrain in integrating fat-free mass determined energy needs: An H2 (15) O PET study. *Hum. Brain Mapp.* **36**, 2406–2415
47. Kennedy, G. C. (1953) The role of depot fat in the hypothalamic control of food intake in the rat. *Proc. R. Soc. Lond. B Biol. Sci.* **140**, 578–596
48. Lin, S. J., Kaeberlein, M., Andalis, A. A., Sturtz, L. A., Defossez, P. A., Culotta, V. C., Fink, G. R., and Guarente, L. (2002) Calorie restriction extends Saccharomyces cerevisiae lifespan by increasing respiration. *Nature* **418**, 344–348
49. Slack, C., Foley, A., and Partridge, L. (2012) Activation of AMPK by the putative dietary restriction mimetic metformin is insufficient to extend lifespan in Drosophila. *PLoS One* **7**, e47699
50. Weindruch, R., Walford, R. L., Fligiel, S., and Guthrie, D. (1986) The retardation of aging in mice by dietary restriction: longevity, cancer, immunity and lifetime energy intake. *J. Nutr.* **116**, 641–654
51. Colman, R. J., Anderson, R. M., Johnson, S. C., Kastman, E. K., Kosmatka, K. J., Beasley, T. M., Allison, D. B., Cruzen, C., Simmons, H. A., Kemnitz, J. W., and Weindruch, R. (2009) Caloric restriction delays disease onset and mortality in rhesus monkeys. *Science* **325**, 201–204

Received for publication April 2, 2018.
Accepted for publication June 12, 2018.